Cosmic Research, Vol. 32, No. 1, 1994

OBSERVATIONS OF $^4He^{++}$ IONS IN THE SOLAR WIND

Yu. I. Ermolaev

UDC 523.72

The main results are summarized from an investigation of the characteristics of $^4He^{++}$ ions (α-particles) in the solar wind on the basis of spacecraft measurements. The abundance of helium n_α/n_p in the solar wind is lower on the average than in the solar atmosphere and depends on the type of solar wind streams. A high content of helium is observed in plasma ejected from the solar atmosphere during transient effects and in streams from coronal regions where the magnetic lines of force have a structure of the coronal hole type. A low helium content is observed in the heliospheric current sheet and in streams from regions where the magnetic field has a structure of the coronal streamer type. The processes responsible for the ejection of helium ions from the corona into the interplanetary medium appear to depend strongly on the configuration of the coronal magnetic field. Thermodynamic equilibrium between protons and α-particles does not exist in the solar wind. The transport velocities of α-particles is higher than the proton velocities on the average ($V_\alpha > V_p$), and the temperature ratio of the particles T_α/T_p is close to 4. At a distance of 1 AU the degree of departure from thermodynamic equilibrium is observed to be related to the types of solar wind streams, the greatest deviation being recorded in streams from regions with a magnetic field structure of the coronal hole type. Observations at various heliocentric distances show that the principal mechanisms of thermodynamic disequilibrium between the components tend to be in effect close to the sun ($r < 0.3$ AU), and the resulting velocity and temperature differences decrease with increasing heliocentric distance.

INTRODUCTION

One of the first direct observations of the solar wind from spacecraft showed that the composition of the solar wind includes not only electrons and protons, but also doubly-ionized helium atoms $^4He^{++}$ (α-particles), whose abundance constitutes an average of approximately 5% of the number of protons [1, 2]. Interest in the study of helium ions in the solar wind has not abated since that time [3–5]. This preoccupation stems primarily from two facts. First, the abundance of helium under diverse conditions in the solar wind provides valuable information about the conditions and possible mechanisms underlying the formation of the wind in the solar corona. Such information has very important bearing on the investigation of the more general, and as yet unsolved, problem of solar corona heating and the generation of the solar wind. Second, because of their low abundance, helium ions can be regarded as test particles for the investigation of physical processes in the interplanetary plasma.

It should be noted that singly ionized helium atoms $^4He^+$ and its doubly ionized isotopes $^3He^{++}$ are also observed in the solar wind. The analysis of the results of measurements of $^4He^+$ and $^3He^{++}$ ions is beyond the scope of the present article. We shall therefore confine the discussion to a few general remarks. First of all, the presence of $^4He^+$ ions in the solar wind is a comparatively rare event: The ratio of the number of $^4He^+$ to $^4He^{++}$ ions at a solar corona temperature above 10^6 K should be $\sim 10^{-6}$ [6], which is beyond the resolution of the instruments used. On the other hand, several events involving a relative content $^4He^+/^4He^{++}$ from 10^{-3} to 0.3 have been detected in the solar wind under certain fairly specific conditions [7–11]. It has been hypothesized in these studies that the observed phenomenon is attributable to the fact that the instruments were picking up the plasma of the cold (10^4–10^5 K) chromosphere of the sun as screening by the magnetic field enabled it to cut through the hot corona during transient processes on the sun (flares, ejections of coronal mass, etc.) before it could alter the ionized state of the ions. Second, measurements performed with the latest high-resolution instruments with good ion selectivity indicate that the helium isotope $^3He^{++}$ is present in the solar wind at all times in an abundance $\sim 4 \cdot 10^{-4}$ relative to $^4He^{++}$ ions [12]. Under ordinary conditions, therefore, helium atoms exist preponderantly in the $^4He^{++}$ state in the solar wind. Accordingly, all subsequent references to helium ions will be understood to mean $^4He^{++}$ ions.

Institute of Space Research, Russian Academy of Sciences. Translated from Kosmicheskie Issledovaniya, Vol. 32, No. 1, pp. 93–125, January–February, 1994. Original article submitted April 23, 1993.

0010-9525/94/3201-0078$12.50

Various types of instruments used to detect α-particles in the solar wind are described in sufficient detail in [3, 13]. The simplest instruments – electrostatic analyzers and Faraday cylinders – were used for the most part in the earliest outer space experiments, but they were not as reliable in differentiating between ion components. A wealth of data have been published from the Explorer 34, ISEE-3, and Prognoz-7, 8 spacecraft using electromagnetic separators (Wien filters), which are capable of discriminating ions by their mass–charge ratio M/q (see [3, 13] and the original papers [14–16]).

The need for high accuracy in the determination of various parameters of the ion components of the solar wind imposes conflicting requirements on the instruments. On the one hand, to increase the accuracy of flux or concentration (particle density) determinations, an instrument must be capable of measuring as large a part of the distribution function of the given ion component as possible. On the other hand, the accurate determination of velocity and temperature requires detailed measurements (i.e., measurements within narrow angular and energy intervals) of the distribution function. These contradictory demands can be reconciled in some cases by increasing the number of measurements of individual fragments of the distribution function. In other cases, however, such attempts are encumbered with major difficulties. The problem is that the majority of spacecraft rotate about an axis perpendicular to the plane of the ecliptic, and instruments with a narrow directivity pattern can scan an angular range in the ecliptic by virtue of the vehicle's rotation. At the same time, some spacecraft (including those of the Prognoz series) have their rotation axis directed toward the sun, or the vehicle maintains a constant triaxial orientation for long time intervals. A highly directional instrument loses any angular scanning capability in these cases, so that the energy distribution of the ions is measured only along the earth–sun line. As a consequence, the uncertainty of measurements of the helium abundance n_α/n_p (n_p is the density of protons) is high, and it is impossible to determine certain directional parameters, specifically the vector velocity difference between α-particles and protons $\mathbf{V}_\alpha - \mathbf{V}_p$. In certain experiments using an instrument with a narrow directivity pattern the estimated abundance can differ from the true value by a factor of ~ 2 or more, in which case only averages can be given by representative estimates of the abundance of the given ion species. The errors of determination of the transport velocity and kinetic temperature are smaller, amounting to (2–10)% and (20–50)%, respectively. It is important to be aware of the additional problem of intercalibration of the measurement results, which shows up as systematic discrepancies between measurements performed by different instruments (on board the same or different spacecraft) in application to the same phenomena; this problem needs to be taken into account in comparing the results of measurements for different instruments [13].

In this article we summarize the main experimental results pertaining to large-scale variations of the parameters of helium $^4He^{++}$ ions (α-particles) in the solar wind. Theoretical information is used only insofar as needed for the interpretation of data.

1. ABUNDANCE OF HELIUM

The physical processes responsible for the ejection of α-particles (and other heavier ions) from the solar atmosphere into interplanetary space constitute one of the remaining unsolved problems of solar wind physics (see the surveys in [5, 17, 18]). Attempts are made to solve the problem by analyzing the results of measurements of the abundance of α-particles relative to protons n_α/n_p in time scales ranging from ~ 1 h to several years. The first time scale characterizes large-scale inhomogeneities of the solar corona, and the other extreme is typical of the global restructuring of the sun in the solar activity cycle. We now examine the results of measurements, first in the smallest and subsequently in the largest time scale.

1.1. Variations of Helium Abundance in the Solar Cycle

So far data have been published on the abundance of helium during the period from 1962 through 1982, spanning almost two 11-year solar activity cycles. The unaveraged values of the α-particle abundance are observed over a fairly broad range of values. According to measurements on board the Vela 3 satellite, for example, this parameters has been observed from 0.081% to 41.7% [19], i.e., within an almost 500-fold range of variation. Data from such measurements often appear in the form of random fluctuations exceeding the uncertainty of the experiments. They can therefore be regarded as evidence in favor of the hypothesis that the corona can be heated (with the effective acceleration of the solar wind) as a result of the relaxation of ion beams as the photospheric magnetic field ascends into the chromosphere and

TABLE 1. Average Helium Abundances in the Solar Wind

Spacecraft	Period (month–year)	n_α/n_p	Source (by Ref. No.)	Remarks
Mariner-2	VIII.62—XII.62	4,6 ± 3,8	2. Neugebauer & Snyder, 1966	
Vela-3	VII.65—VIII.65	4,2	23. Hundhausen et al., 1967	
Explorer-34	V.67—I.68	5,1 ± 2,0	14. Ogilvie & Wilkerson, 1969	
Heos-1	XII.68—III.69	5,5 ± 0,5	24. Formisano et al., 1970	
Vela-3	VII.65—VIII.65	4,3	19. Robbins et al., 1970	
	VII.65—VII.67	3,7 ± 2,6		
Vela-3	VII.65—VII.66	3,4	25. Hirshberg et al., 1972	
	VII.66—VII.67	4,3		
Explorer-43	III.71—IV.71	4,2	26. Ogilvie, 1972	
Heos-1	XII.68—IV.70	~5,2	27. Moreno & Palmiotto, 1973	Estimated from Fig. 1
Mariner-2	VIII.62—XII.62	3,2 ± 1,0	28. Ogilvie & Hirshberg, 1974	*
Vela-3	VII.65—III.66	3,4 ± 0,4		Quiet SW**
	III.66—VII.67	3,9 ± 0,4		Disturbed SW
Explorer-34	V.67—I.68	$5{,}1^{+0{,}0}_{-1{,}0}$		*
OGO-5	III.68—IV.69	4,6 ± 1,0		
Heos-1	XII.68—IV.70	<5,1		*
Explorer-43	III.71—IV.71	4,7 ± 0,7		*
Apollo-15	VIII.71—VI.72	4,1		
IMP-6—8	III.71—VII.74	3,8 ± 1,8	29. Bame et al., 1977	V < 350 km/sec***
		4,8 ± 0,5		V > 350 km/sec
IMP-6—8	III.71—I.77	3,1—5,3	30. Feldman et al., 1978	
Helios-1	XII.74—II.82	1,1—5,5	31. Schwenn, 1983	
Prognoz-7	XI.78—VII.79	5,4 ± 3,9	5. Ermolaev, 1987	
Prognoz-7	XI.78—VII.79	3,0 ± 2,8	33. Ermolaev et al., 1988	$T_p \geq 3 \cdot 10^5$ K
ISEE-3	VIII.78—XII.78	3,2 ± 3,9	34. Ogilvie et al., 1989	V < 450 km/sec
		4,5 ± 6,0		V >450 km/sec
		3,5		For all V
	I.79—VI.79	4,4 ± 5,4		V < 450 km/sec
		5,6 ± 5,4		V >450 km/sec
		5,0		For all V
	VII.79—XII.79	5,3 ± 5,0		V < 450 km/sec
		5,5 ± 4,5		V >450 km/sec
		5,3		For all V
	I.80—VI.80	3,7 ± 5,0		V < 450 km/sec
		3,9 ± 4,0		V >450 km/sec
		3,8		For all V
	VII.80—XII.80	3,5 ± 4,5		V < 450 km/sec
		4,0 ± 5,3		V >450 km/sec
		3,7		For all V
	I.81—VI.81	4,0 ± 5,0		V < 450 km/sec
		4,9 ± 6,0		V >450 km/sec
		4,2		For all V
	VII.81—XII.81	4,0 ± 4,0		V < 450 km/sec
		4,5 ± 3,5		V >450 km/sec
		4,1		For all V
	I.82—VI.82	3,1 ± 2,0		V < 450 km/sec
		4,1 ± 2,0		V >450 km/sec
		3,6		For all V
	VII.82—XII.82	3,0 ± 1,8		V < 450 km/sec
		3,8 ± 2,3		V >450 km/sec
		3,5		For all V
	VIII.78—XII.82	3,8 ± 4,0		V < 450 km/sec
		4,5 ± 4,3		V >450 km/sec
		4,1		For all V
Prognoz-8	I.81—VIII.81	3.7 ± 4.3	Unpublished	

*These data were obtained with allowance for the operational methodological characteristics of the instruments and differ from those obtained earlier.

**The abbreviation SW stands for "solar wind."

***The symbol V denotes solar wind speed.

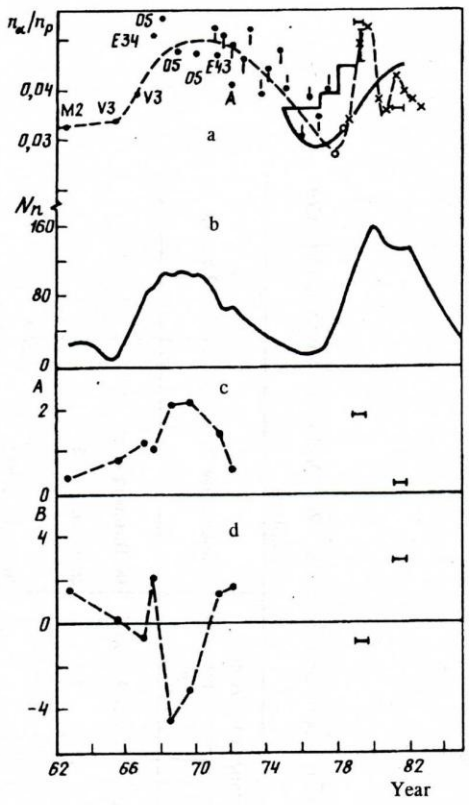

Fig. 1. Long-term variations of helium abundance according to spacecraft measurements (a), number of sunspots N_s (b), and linear regression coefficients A (c) and B (d) (see text).

rejoins the coronal magnetic field [20]. By this mechanism the helium abundance in the beams can be the same as in the photosphere, i.e., higher than in the surrounding coronal plasma. It is important to note, however, that the maximum values observed in the solar wind are much greater than the estimates of the average helium abundance in the solar atmosphere (6-16% [21]).

After the data are averaged over a time interval comparable with the sun's period of rotation (27 days), the helium abundances obtained on different spacecraft change comparatively little and are equal to (3–6)% (see Table 1). On the whole, the average abundances of α-particles in the solar wind are lower than the lowest estimate of the helium abundance on the sun's surface $(6.3 \pm 1.5)\%$ [22] and in the solar atmosphere $\sim 6\%$ [21].

The existence of long-period variations of the helium abundance in the solar wind during the solar activity cycle has been hypothesized in [19, 24] and later corroborated in numerous experiments [3, 5, 26, 28, 31, 32, 34–37]. In particular, it has been shown [34] on the basis of data from ten spacecraft during 1962–82 that the variation of the α-particle abundance can be correlated with the number of sunspots (see Fig. 1). The dots in Fig. 1a indicate the results of measurements on different spacecraft: Mariner 2 (point *M2*), Vela 3 (*V3*), Explorer 34 and 43 (*E34* and *E43*), OGO 5 (*O5*), Apollo 15 (*A*), IMP 6–8 (*I*) according to [3]; the crosses represent ISEE 3 measurements, the light circles correspond to Voyager 2, and the dashed curve is the result of smoothing the above-cited data [34]. Also shown are yearly-average data for 1975–78 [32] from the IMP 6–8 satellites [32] (stairstep curve, where the lengths of the horizontal segments correspond to the averaging intervals), from the Helios 1 (December 1974 through February 1982) and Helios 2 (January 1976 through March 1980) satellites [31] (solid curve), and from the Prognoz-7 (November 1978 through June 1979) [5] and Prognoz-8 (January–August 1981) satellites (segments of length equal to the averaging interval). Despite the appreciable scatter of the measured abundances, a distinct time correlation with the number of sunspots is evident (Fig. 1b).

TABLE 2. Approximate Relations Expressing the Dependence of Helium Abundance on Solar Wind Velocity, Temperature, Concentration, and Flux

Spacecraft	Period (month–year)	Approximation	Approximation coefficients		Source (by Ref. No.)	Remarks
			A	B		
Vela-3	VII.65—VIII.65	$n_\alpha/n_p = A(V \times 10^2) + B$	1,02 ± 0,03	−0,39 ± 0,14	38. Hirshberg et al., 1972	
Explorer-34	V.67—I.68		1,08	2,2	26. Ogilvie, 1972	
Explorer-43	III.71—IV.71		0,90	1,37		
Vela-3	VII.65—VIII.65	$n_\alpha/n_p = A(T^{1/2}[10^3\mathrm{K}]) + B$			26. Ogilvie, 1972	
Explorer-34	V.67—I.68		0,28	—		From three spacecraft
Explorer-43	III.71—IV.71					
Heos-1	XII.68—III.69	$n_\alpha/n_p = A(V \times 10^2) + B$	2,2	−3,25	27. Moreno & Palmiotto, 1973	
Mariner-2	VIII.62—XII.62		0,35	1,6	28. Ogilvie & Hirshberg, 1974	*
Vela-3	VII.65—VIII.66		0,8	0,2		Quiet SW
	III.66—II.67		1,2	−0,7		Disturbed SW
OGO-5	III.68—IV.69		2,1	−4,5		
Heos-1	XII.68—IV.70		2,2	−3,2		*
Explorer-43	III.71—IV.71		1,4	1,4		*
Apollo-15	VIII.71—VI.72		0,57	1,7		

Prognoz-7	XI.78—VII.79		1,9	−0,7	Unpublished	All data
			8,0 ± 0,5	−22,4 ± 1,6		Type 2 SW
			0,5 ± 0,3	6,7 ± 1,3		Type 3 SW
		$n_\alpha/n_p = 10^A V^B$	−4,95 ± 0,17	2,1 ± 0,3		All data
			—	7,06		Type 2 SW
			—	0,54		Type 3 SW
		$n_\alpha/n_p = 10^A T^B$	0,40 ± 0,02	0,21 ± 0,02		All data
			—	0,62		Type 2 SW
			—	−0,44		Type 3 SW
		$n_\alpha/n_p = 10^A n^B$	1,08 ± 0,02	−0,59 ± 0,02		All data
			—	−1,18		Type 2 SW
			—	0,15		Type 3 SW
		$n_\alpha/n_p = A(nV \times 10^8) + B$	−0,37 ± 0,07	6,7 ± 0,2		All data
			−0,93	9,5		Type 2 SW
			0,27	8,4		Type 3 SW
		$n_\alpha/n_p = 10^A (nV)^B$	1,42 ± 0,06	−0,56 ± 0,08		All data
		—	—	−0,84		Type 2 SW
		—	—	0,20		Type 3 SW
Prognoz-8	I.81—VIII.81	$n_\alpha/n_p = A(V \times 10^2) + B$	0,2	3,0	Unpublished	

*These data were obtained with allowance for the operational methodological characteristics of the instruments and differ from those obtained earlier.

According to Vela 3 satellite data, a positive correlation is observed between the abundance of α-particles and the solar wind velocity V_p [19]; the linear regression coefficients of these parameters has been determined in [26–28, 38] (see Table 2). Two hypothesis have been analyzed [28] on the basis of the results of several experiments during 1962–72: 1) the average abundance of α-particles increases with the number of sunspots in the solar activity cycle, independently of the solar wind velocity (i.e., the free term B increases in the linear function $n_\alpha/n_p = AV_p + B$); 2) the number of events accompanied by the observation of high-velocity streams with elevated helium abundances (i.e., an increase in the linear regression coefficient A) increases at the solar activity maximum, and it has been noted that the coefficient A correlates with the number of sunspots. The variations of the coefficients A and B in Figs. 1c and 1d (see Table 2) support the conclusion that a correlation exists between the coefficient A and the number of sunspots. The anticorrelation of the coefficient B with the number of sunspots in Fig. 1d is probably of minor consequence, merely reflecting the linear relation between the number of sunspots and the coefficient A.

The solar-cycle variations of the velocity dependence of the helium abundance have been investigated indirectly according to IMP 6–8 satellite data [30], where the helium abundances were compared in streams with velocities $V_p < 350$ km/sec and $V_p > 600$ km/sec. An analysis of these parameters suggested that the maximum difference between the helium abundances in fast and slow solar wind streams in the period 1971–76 (in the downturn phase of solar activity) is observed near the minimum of the solar cycle. According to ISEE 3 spacecraft data [34], the minimum difference in the helium abundances in 600-km/sec and 300-km/sec streams during the period 1978–82 was observed in the maximum solar activity phase.

The reason for the differences of the IMP 6–8 and ISEE 3 results from previous observations could well be the different procedure used to analyze the data. First, a large part of the data was excluded from the analysis (e.g., according to Prognoz-7 satellite measurements, more than 80% of the data lie in velocity range 350–600 km/sec). This fact artificially elevates the role of certain types of solar wind streams that would play a minor role in calculating the linear dependence from the complete set of data. Second, data obtained in the velocity range where different types of streams are observed were analyzed in the presence of small statistics, so that the parameters can vary considerably. Under these conditions it should be required to investigate the solar-cycle variations of the number of different types of solar wind streams and the average helium abundances for each of them.

1.2. Relationship of Helium Abundance to Solar Wind Parameters

The variations in the chemical composition of the solar wind in a time scale of the order of one hour or more are most likely attributable to specific mechanisms responsible for the ejection of coronal plasma into interplanetary space. The sum-total result of the action of these mechanisms is determined by the conditions in the region where the solar wind originates, at a distance of several sun radii. These conditions, in turn, can be patently manifested in the solar wind parameters at a distance of 1 AU from the sun. Consequently, a comparison of the results of helium abundance measurements at 1 AU with the hydrodynamic parameters of the stream can yield important information as to which conditions (and mechanisms) in the region of formation of the solar wind promote or inhibit the ejection of small ion components into interplanetary space.

The dependence of the helium abundance on the velocity V_p and flux nV_p of the solar wind (n is the total density of particles) has been studied the most thoroughly to date. Figure 2a shows graphs of n_α/n_p as a function of V_p, determined from measurements on board the satellites Vela 3 [25] (curve *V*3), Explorer 34 and 43 [26] (*E*34 and *E*43), Heos 1 [27] (*H*1), IMP 6–8 [29] (*I*6–8), OGO 5 [3] (*O*5), and Prognoz-7 [39, 40] (circles П7). Figures 2b and 2c show the same dependence averaged over semiannual intervals during 1978–82 according to ISEE 3 data [34]. The dot–dash line in Fig. 2c is drawn to approximate Vela 3 satellite data [38]. On the average, the results of all the experiments exhibit satisfactory agreement and indicate that the helium abundance increases with the solar wind velocity.

As mentioned above, the data of some of the experiments represented in the figure have been approximated by linear functions (see Table 2). However, it is evident from the figure that the graphs of the helium abundance as a function of velocity behave not only nonlinearly (e.g., the Prognoz-7 satellite data are best approximated by the function $V_p^{2.1\pm0.3}$ [39]), but also nonmonotonically. In our opinion, this can be attributed to the fact that the given dependence can differ

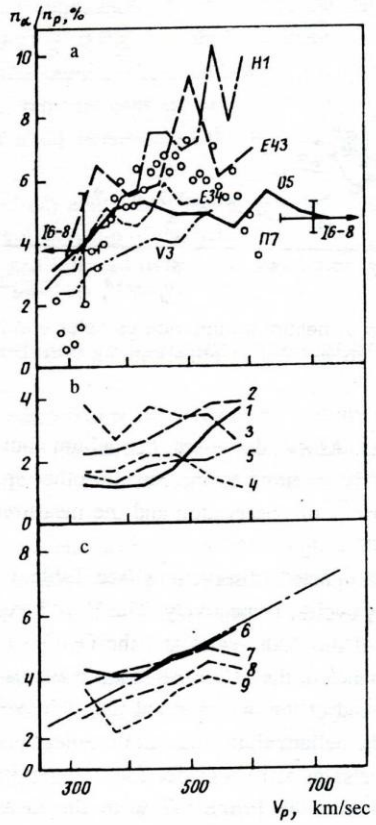

Fig. 2. Average graphs of helium abundance vs solar wind velocity according to: a) measurements on nine satellite; b, c) ISEE 3 measurements (see text).

in different types of solar wind streams, whose frequency of occurrence probably varies within the solar cycle, and after averaging over a long time interval the resultant dependence is determined by the particular set of measurement periods with different types of streams occurring in this time interval.

One of the possible physical processes affecting the ejection of heavy ions from the solar corona into interplanetary space is their Coulomb friction with the main – i.e., proton – component of the plasma. In particular, it has been suggested [41] on the basis of a theoretical investigation that there is a minimum plasma flux threshold, above which heavier-than-proton ions must eject quite efficiently into interplanetary space. On the other hand, Gosling et al. [42] have proposed an empirical model based on measurements from satellites of the Vela and IMP series, whereby the helium abundance in streams originating from coronal streamers decreases, while the ion density increases as the spacecraft approaches the core of the streamer and the heliospheric current sheet, i.e., an anticorrelation is observed between the helium abundance and the concentration (flux) of the solar wind. Of special interest in this regard are the graphs in Fig. 3, which show the helium abundance as a function of the solar wind flux in Fig. 3 according to the results of observations on board the Vela 3 [25] (*V*3), Explorer 34 and 43 (*E*34 and *E*43), Heos 1 [27] (*H*1), OGO 5 [3] (*0*F), and Prognoz-7 [39, 40] (П7).

In dense streams with $nV_p > 3 \cdot 10^8$ cm^{-2}·sec^{-1} the data of all space experiments are in mutual agreement and indicate a decrease in the helium abundance as the flux increases. The disparities between the results of different space experiments are substantial in less dense streams with $nV_p < 3 \cdot 10^8$ cm^{-2}·sec^{-1}. Not to be overlooked, of course, is the possibility that the experimental errors of determination of the abundance of α-particles in such streams are so high that they exceed the observed differences. However, it would be impossible not to call attention to the qualitative difference

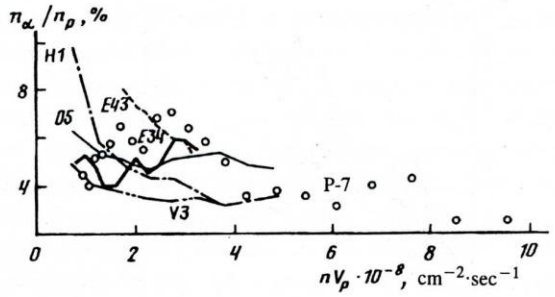

Fig. 3. Average graphs of helium abundance vs solar wind flux according to spacecraft observations.

in behavior between two groups of experiments: As nV_p decreases, the helium abundance n_α/n_p is observed to decrease on the Explorer 34 and Prognoz-7 satellites, but is observed to increase on other spacecraft. At least two differences exist between these groups of experiments: the periods of observation and the measurement procedures. Let us consider each one in detail.

The periods of the Explorer 34 and Prognoz-7 observations (see Table 1 and Fig. 1) occurred at the end of the upturn phase of the 20th and 21st solar activity cycles, respectively. The Vela 3 experiments closest in time to those on the Explorer 34 (beginning of the upturn phase of the 20th cycle) and the OGO 5 (beginning of the maximum of the 20th cycle) indicate an extremely weak flux dependence of the helium abundance at small fluxes. On the other hand, the Heos 1 and Explorer 43 experiments occurred at the end of the maximum of the 20th cycle and indicate a steep dependence. We can therefore assume that the dependence of the helium abundance on the solar wind flux at small values of the latter is apt to undergo a qualitative change (of sign) in the solar activity cycle. This assumption is in need of further investigation.

Moreover, only on the Explorer 34 and the Prognoz-7 were the measurements performed by mass-analytic techniques [14, 16], which can yield more reliable separation of protons and α-particles. All other data were obtained by energy-analytic methods, which can give excessive estimates for the α-particle flux in weak and hot solar wind streams because of the significant contribution of protons to the energy distribution of α-particles. In this case the results of the Explorer 34 and Prognoz-7 measurements in low-flux streams support the hypothesis [41] that small ion components are drawn from the solar corona into interplanetary space by virtue of their Coulomb friction with the proton component [40, 43]. However, this hypothesis requires further investigation as well.

The dependence of the helium abundance on the proton concentration (number density of protons) of the solar wind has been investigated [14] according to data from the Explorer 34 satellite. These experimental data show that n_α/n_p decreases as n_p increases. At a later time, Heos 1 data failed to disclose any such functional relation between the helium abundance and the concentration of the solar wind [24]. As mentioned above, according to data from the Vela and IMP series satellites, the helium abundance has been observed to decrease with increasing concentration in dense and slow solar wind streams [42, 44]. According to Prognoz-7 data, this dependence is not monotonic: n_α/n_p increases from 4.5% to 6.5% as n_p increases from 2 cm^{-3} to 4 cm^{-3}, remains constant in the interval 4–7 cm^{-3}, and decreases to $\sim 1\%$ when n_p increases to 50 cm^{-3}. This trend in the variation of the helium abundance persists for the most part after the additional selective sampling of velocity and temperature data [40].

On the whole, the concentration dependence of the helium abundance is similar to its flux dependence. This similarity is attributable to the fact that the variation of the proton concentration is stronger on the average than the velocity variation (numerous experiments indicate an average dependence $n_p \sim V_p^{-2}$; see, e.g., [5, 45] and the references cited therein), so that the flux mirrors the behavior of the concentration to a greater degree than the velocity of the solar wind.

An indirect estimate of the dependence of the helium abundance on the temperature T_p of solar wind protons has been obtained [26] on the basis of Vela 3 and Explorer 34 and 43 data. The authors of this paper first determined a linear relation between the helium abundance and the velocity (see Table 2) and then obtained the following functional dependence on the basis of the temperature–velocity relation of the solar wind [46]: $(n_\alpha/n_p)\cdot 10^2 = 0.28(T_p[10^3\ \mathrm{K}])^{1/2} + f$, where f is a weak function of the solar activity. The Prognoz-7 data demonstrate a more complex behavior on the part of

the temperature dependence of the helium abundance. In particular, the data are best approximated when the power exponent of the temperature is equal to 0.21 ± 0.02, i.e., the dependence is not as steep, on the whole, as determined earlier. However, this dependence is not monotonic. The abundance n_α/n_p increases from ~4% to ~6% as the temperature increases in the interval $(1\text{–}4)\cdot 10^4$ K, remains constant at this level up to $10\cdot 10^4$ K, and decreases to 2% when the temperature increases to $50\cdot 10^4$ K. This trend persists, on the whole, after the additional selective sampling of both velocity and concentration data [40].

The observed variations of the helium abundance as the hydrodynamic parameters of the solar wind vary point conclusively to the existence of a definite relationship of the helium abundance to the condition and types of streams of the solar wind; this relationship will be discussed in detail in the next subsection.

1.3. Helium Abundance in Different Types of Solar Wind Streams

Important information about the mechanisms underlying the evolution of the chemical composition of the solar wind can be obtained from a comparison of the helium abundance with the known types of solar wind streams, which can – with a certain degree of reliability – be correlated with the large-scale structure of the solar corona and the dynamical effects taking place in them.

The results of myriad space experiments have shown that a significant increase in the helium abundance (two or three times the average) is observed in streams formed by solar flares and detected after the incidence of interplanetary shock waves on the vehicles; such streams are sometimes accompanied by the sudden onset of geomagnetic storms [14, 25, 47–50]. Certain events involving an increase in the helium abundance to 10% or more have been identified with the injection of coronal mass during transients and also with radio bursts of the second and fourth types [51]. The slight increase in the helium abundance in high-velocities solar wind streams can be attributed to plasma flowing out of regions in which the lines of force of the coronal magnetic field have a structure of the coronal hole type [29].

It has been shown on the basis of measurements on satellites of the Vela and IMP series that the lowest helium abundance is observed in dense and slow streams originating in coronal streamers and in the heliospheric current sheet, which separates a streamer into parts with oppositely oriented interplanetary magnetic fields [42, 44, 51].

Developing earlier conclusions and drawing on IMP 6–8 data, Bame [32] has investigated the dependence of the hydrodynamic parameters of the solar wind on the helium abundance and has shown that solar wind streams can be classified by type (low-velocity, high-velocity, and flare-derived streams) in order of increasing value of n_α/n_p.

The patterns of variation of the parameters of α-particles relative to protons in the region of interaction between high-velocity and low-velocity streams have been investigated by the epoch-superposition method according to Vela series [52] and IMP series [53] satellite data. It was shown that the helium abundance at the interface of streams with different velocities does not change appreciably, on the average, from the abundance in the streams themselves.

Five distinct regions of the concentration–velocity plane have been distinguished (see Fig. 4 and Table 3) on the basis of the variations of several solar wind parameters measured on the Prognoz-7 satellite [n_p, V_p, n_α/n_p, and $\beta = nT_p/(B^2/8\pi)$, where k is the Boltzmann constant, and B is the modulus of the magnetic field]. Judging from previous results, we have advanced the hypothesis that these regions of the plane (i.e., a certain relation between abundance and velocity, which in combination determine the kinetic energy of a solar wind stream) are associated with the well-known large-scale structure of the solar corona and with dynamic phenomena in them: 1) the heliospheric current sheet; 2) streams emanating from coronal streamers; 3) streams from coronal holes; 4) disturbed streams at large angular distances from the axis of transient phenomena in the solar corona; 5) disturbed streams at small angular distances from transient phenomena in the corona, including the so-called piston and/or plasma ejected from the solar atmosphere during this event [43, 54]. Figure 4a shows schematically the structure of the magnetic field in the ecliptic near the sun and the associated types of solar wind streams; Figs. 4a and 4b show the distributions of the types of streams (a) and the helium abundances and fluxes of the solar wind (b), all on the concentration–velocity plane. On the whole, these results are consistent with previously measured dependences of the helium abundance on the velocity and flux nV_p and with the observed relationship between the helium abundance and the types of streams in the solar wind. We have thus proposed a quantitative criterion for classifying the types of solar wind streams, the distribution of the helium abundance by these types of streams, and their relationship to the structure and dynamics of the solar corona.

TABLE 3. Average Solar Wind Parameters and Their Variations with Increasing Concentration and Velocity in Five Types of Solar Wind According to Prognoz-7 Measurements

SW type	Fraction, %	V_p, km/sec		n, cm^{-3}		B, nT			T_p, 10^4 K			β			n_α/n_p, %		
		interval	average	interval	average	average	n	V	average	n	V	average	n	V	average	n	V
1	8	270 – 450	351 ± 45	15 – 20	29,6 ± 10	6,3 ± 2,3	↘	↗	5,4 ± 4,4	↘	↗	2,0 ± 1,7	?	↗	1,7 ± 1,5	↘	↗
2	33	270 – 470	359 ± 33	3 – 30	9,6 ± 4,2	7,2 ± 3,0	↗	↗	5,4 ± 5,1	—	↗	0,5 ± 0,5	—	↗	4,4 ± 4,0	↘	↗
3	49	380 – 630	449 ± 52	2 – 30	6,1 ± 3,4	6,9 ± 2,7	↗	—	9,8 ± 8,5	—	↗	0,5 ± 0,6	↗	—	5,5 ± 6,0	↗	↗
4	6	450 – 700	573 ± 79	3 – 30	8,3 ± 7,9	9,5 ± 3,5	↗	↗	14,6 ± 12,5	—	↗	0,6 ± 0,5	↗	—	3,5 ± 3,5	?	↘
5	4	480 – 700	515 ± 44	3 – 40	8,6 ± 5,5	11,4 ± 8,0	↗	↗	18,8 ± 14,1	—	↗	1,0 ± 0,8	—	—	4,8 ± 4,6	?	↘

The arrows and in the n and V columns indicate that B, T_p, β, or n_α/n_p increases or decreases (respectively) as the concentration (total particle density) and velocity increase.

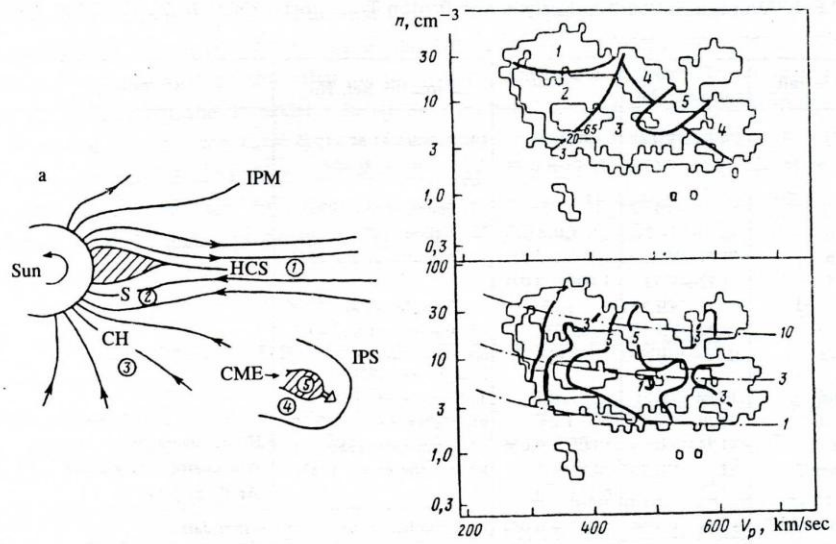

Fig. 4. a) Large-scale structure of the coronal magnetic field and associated types of solar wind (see text); b, c) distribution maps on the $n - V_p$ plane (the thin lines demarcate zones with >3, >20, and >65 measurements in the unit cell): a) five types of solar wind; b) helium abundance (solid curves, in %) and solar wind flux (dot–dash curves, in units of 10^8 $cm^{-2} \cdot sec^{-1}$). Notation: IPM) interplanetary magnetic field; HCS) heliospheric current sheet; S) streamer; CH) coronal hole; CME) coronal mass ejection; IPS) interplanetary shock.

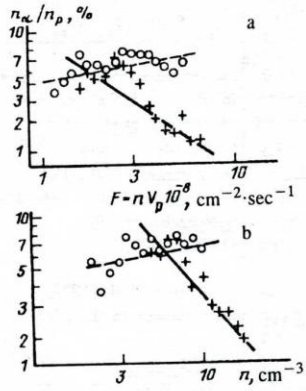

Fig. 5. Average graphs of helium abundance vs flux (a) and concentration (b) for streams originating from streamers (the average abundances are represented by ×'s, and the results of approximation by solid lines) and streams from coronal holes (circles and dashed lines) according to Prognoz-7 data.

This classification of the solar wind streams permits the dependence of the helium abundance on the hydrodynamic parameters to be investigated separately for each of the different types of streams. Figure 5 shows the helium abundance as a function of the flux and concentration. Clearly, not only do these dependences have different slopes, but even the signs of the slopes differ in different types of streams, which is in good agreement with our conclusions in the preceding chapter. However, since this approach has been used strictly for data from a single experiment, it is required, first of all, to confirm the conclusions and, second, to investigate the variations in the solar activity cycle; measurements on other spacecraft can be used for this purpose.

TABLE 4. Average Ratios of α-Particle and Proton Transport Velocities V_α/V_p in the Solar Wind

Spacecraft	Period (month–year)	V_α/V_p	Source (by Ref. No.)	Remarks
Vela-3	VII.65—VII.67	1,02 ± 0,03	19. Robbins et al., 1970	
Explorer-34	V.67—I.68	1,004 ± 0,03	55. Ogilvie & Zwally, 1972	
Heos-1	XII.68—III.69	1,02	35. Bollea et al., 1972	
IMP-6	III.71—IV.71	1,018	56. Ogilvie, 1975	
IMP-6	III.71—VII.72	1.001 (±0,02)	57. Asbridge et al., 1976	
IMP-7	I.73—V.73	1,007 (±0,02)		
Prognoz-1	IV.72—VII.72	1,03	58. Zertsalov et al., 1976	
Prognoz-1	IV.72—VII.72	1,035	59. Bosqued et al., 1977	
Heos-2	II.72—VIII.74	1,004	60. Grünwaldt & Rosenbauer, 1978	
OGO-5	III.68—IV.71	1,012	3. Neugebauer, 1981	
ISEE-3	II.79—IV.79	1,04	61. Ogilvie et al., 1982	
Prognoz-7	XI.78—VII.79	1,005 ± 0,055	62. Ermolaev, 1986	Hourly averages
Prognoz-7	XI.78—VII.79	0,96 ± 0,04	63. Avanov et al., 1987	Post-interplanetary shock
		0,998 ± 0,076		At $T_p > 3 \cdot 10^5$ K
Prognoz-7	XI.78—VII.79	1,007 ± 0,054	33. Ermolaev et al., 1988	4-min data
Prognoz-8	I.81—VIII.81	0,997 ± 0,050	Unpublished	
Prognoz-7	XI.78—VII.79	1,003	Unpublished	1 type 1 SW
		0,997		2 type 2 SW
		1,017		3 type 3 SW
		0,96		4 type 4 SW
		1,012		5 type 5 SW

TABLE 5. Average Ratios of α-Particle and Proton Kinetic Temperatures in the Solar Wind

Spacecraft	Period (month–year)	T_α/T_p	Source (by Ref. No.)	Remarks
Explorer-34	VI.67—XII.67	1,6—5,0	14. Ogilvie & Wilkerson, 1969	
Explorer-34	VI.67—XII.67	3,75	46. Burlaga & Ogilvie, 1970	
Vela-3	VII.65—VII.67	4,02 ± 2,5	19. Robbins et al., 1970	
Explorer-34	V.67—I.68	3,0 ± 1,0	55. Ogilvie & Zwally, 1972	
Prognoz-1	IV.72—VII.72	3,6	58. Zertsalov et al., 1976	
Prognoz-1	IV.72—VII.72	3,83	59. Bosqued et al., 1977	
OGO-5	III.68—IV.71	4,87	3. Neugebauer, 1981	
Prognoz-7	XI.78—VI.79	4,2 ± 2,8	62. Ermolaev, 1986	Hourly averages
				Post-interplanetary shock
Prognoz-7	XI.78—VI.79	3,0 ± 1,2	63. Avanov et al., 1987	
		4,3 ± 2,8	33. Ermolaev et al., 1988	4-min data
		2,7 ± 1,7		At $T_p > 3 \cdot 10^5$ K
Prognoz-8	I.81—VIII.81	4,2 ± 2,6	Unpublished	
Prognoz-7	XI.78—VI.79	2,7 ± 2,8	Unpublished	1 type 1 SW
		4,2 ± 3,3		2 type 2 SW
		4,4 ± 3,1		3 type 3 SW
		3,6 ± 3,0		4 type 4 SW
		4,3 ± 3,0		5 type 5 SW

2. VELOCITY AND TEMPERATURE OF HELIUM IONS

In contrast with the abundance of helium, its transport velocity V_α and kinetic temperature T_α undergo sizable variations in interplanetary space. Owing to the small number of α-particles (and the difference of their mass and charge

from the proton values), they can be regarded as test particles for investigating the dynamics of the solar wind plasma, where their behavior is logically compared with the variations of the main, i.e., proton, component of the solar wind.

Numerous space experiments have shown that thermodynamic equilibrium between different ion components does not exist in the solar wind: Although the transport velocity of α-particles is close to the proton transport velocity, V_α is slightly higher than V_p on the average (see Table 4), and the kinetic temperature of the α-particles is ~ 4 times the proton temperature on the average (see Table 5). The velocities of other solar wind ions are also somewhat higher, on the average, than the proton velocity and are close to the α-particle velocity [64], while their temperatures T_i exceed the proton temperature by an amount roughly proportional to the ratio of the ion masses, i.e., $T_i \approx (m_i/m_p)T_\mathrm{p}$ [64–66]. This relation implies that the thermal velocities of the different ion components are equal.

2.1. Relationship to the Types of Solar Wind Streams

To obtain information about the mechanisms of the acceleration and heating of solar wind ions, it is important to investigate the relationship of the velocity and temperature of different ions to the different conditions and types of solar wind streams.

As mentioned in the Introduction, measurements of the vector difference in the transport velocities of protons and α-particles $\mathbf{V}_\alpha - \mathbf{V}_p$ are reported in the majority of experiments, while some experiments, including those on satellites of the Prognoz series, involve measurements of the difference in the radial components of the velocity (owing to the permanent orientation of the satellites' axes of rotation toward the sun). Since the vector velocity difference is usually aligned with the magnetic field (or the heat-flux vector [57]), which has the shape of an Archimedean spiral on the average, the scalar velocity difference is ~ 30–40% smaller than the vector velocity difference [3, 62], and this fact must be taken into account in analyzing the data.

The results of Vela 3 [52] and IMP 6–8 [30] satellite measurements have indicated an increase in the α-particle–proton velocity difference $(V_\alpha - V_p)$ in high-velocity streams. On the average, the difference $V_\alpha - V_p$ (or its vector counterpart $\mathbf{V}_\alpha - \mathbf{V}_p$) increases almost monotonically with increasing wind velocity. Figure 6 shows the results of determining the modulus of the vector velocity difference as a function of the proton velocity from IMP 6 and 7 [57], Heos 2 [60], OGO 5, Explorer 43 [3], and Prognoz-7 data [39, 40] (the Prognoz measurements differ from the others in this experiment in that the difference in the radial components of the ion velocities were determined). The satellites are designated by symbols analogous to those in Figs. 1–3. The IMP 6 and 7 data at wind velocities greater than 400 km/sec were approximated by the relation $|\mathbf{V}_\alpha - \mathbf{V}_p| = 0.08V_p - 23$ km/sec or $V_\alpha - V_p = 0.032V_p - 12$ km/sec. ISEE 3 spacecraft observations have shown that the average velocity difference between α-particles and protons is ~ 5 km/sec in the range of solar wind velocities from 300 km/sec to 400 km/sec and ~ 14 km/sec in the range from 400 km/sec to 500 km/sec [61], in agreement with the results of other experiments.

According to IMP 6 satellite data [57], the α-particle–proton velocity difference was compared with the Alfvén velocity during the period 30.III–2.IV 1971, yielding a direct correlation between these parameters (the linear approximation has the form $|\mathbf{V}_\alpha - \mathbf{V}_p| = V_A - 25$ km/sec). This correlation, combined with a series of theoretical models constructed to characterize the predominant acceleration of α-particles by virtue of their interaction with waves, led to the assumption that the Alfvén velocity could serve as a measure of the velocity difference between ions, so that many subsequent papers looked at the behavior of the dimensionless quantity $(V_\alpha - V_p)/V_A$. This problem will be discussed in detail in the next subsection.

Like the velocity difference, the ratio of the temperatures of α-particles and protons T_α/T_p correlates with the transport velocity of the solar wind. Figure 7 shows the average values of the ratio T_α/T_p as a function of the proton velocity for six space experiments: Vela 3 [67], Prognoz-1 [59], Explorer 34 and OGO 5 [3], ISEE 3 [68], and Prognoz-7 [67]. The ISEE 3 data were obtained from the functional dependence of T_α/T_p on $t = R/V_p$ in [68], where the plasma propagation time t was determined as the ratio of the distance $R = 1$ AU to the solar wind velocity. Since the description of the experiment includes the statement that the parameters were measured reliably only up to a velocity of 600 km/sec, the data given for $V_p > 600$ km/sec are probably not reliable.

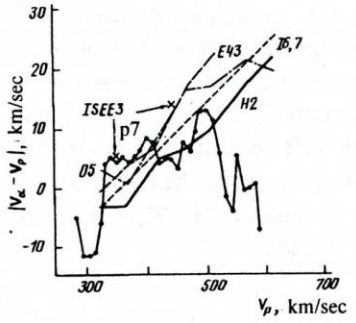

Fig. 6

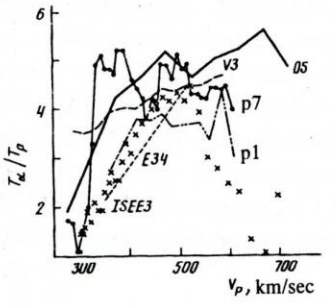

Fig. 7

Fig. 6. Average graphs of the modulus of the α-particle–proton velocity difference $|\mathbf{V}_\alpha - \mathbf{V}_p|$ [3, 57, 60] and the difference in their radial components $V_\alpha - V_p$ vs solar wind velocity. ×) ISEE 3 data.

Fig. 7. Average graphs of the α-particle–proton temperature ratio T_α/T_p vs proton velocity according to spacecraft measurements [3, 39, 40, 59, 67, 68] (the notation is similar to Figs. 1–3).

It has been discovered on the basis of mass spectrometer measurements on the Prognoz-1, 7, and 8 satellites that the α-particle transport velocity can be 50 km/sec lower than the proton velocity, and the temperature ratio of the particles can be <4 behind an interplanetary shock front for a period lasting from a few tens of minutes to several hours [33, 58, 63, 69–73].

Consequently, space experiments have demonstrated conclusively that the velocity difference and temperature ratio between α-particles and protons are small in low-velocity solar wind streams and in streams disturbed by the passage of interplanetary shocks, but they increase in high-velocity streams.

The distributions of the parameters $V_\alpha - V_p$, $(V_\alpha - V_p)/V_A$, T_α/T_p, τ_e/τ_s, and τ_e/τ_s in the concentration–velocity plane, obtained from the results of Prognoz-7 measurements and shown in Fig. 8, present a graphic picture of how these parameters are distributed among the types of solar wind streams. The parameters τ_e/τ_s and τ_s/τ_c are determined from local measurements of the plasma parameters according to the equations [73, 3, 76][1]

$$\tau_e/\tau_c = \text{const}\,\frac{rn\exp(-X^2)}{V_p T_{ef}^{3/2}}, \quad X = \frac{|V_\alpha - V_p|}{[2k(T_p/m_p + T_\alpha/m_\alpha)]^{1/2}}. \tag{1}$$

$$T_{ef} = \frac{m_p T_p + m_\alpha T_\alpha}{m_p + m_\alpha},$$

$$\tau_e/\tau_s = \text{const}\,\frac{rnG(X)}{V_p|V_\alpha - V_p|\,[2k(T_p/m_p + T_\alpha/m_\alpha)]}, \tag{2}$$

where r is the heliocentric distance, $G(X)$ is the error integral, m is the mass, and k is the Boltzmann constant.

A positive velocity difference is detected in streams from coronal holes, where the degree of departure from thermodynamic equilibrium increases with decreasing concentration; this trend is associated with the decrease in the ratio of the flux propagation time τ_e to the characteristic momentum transfer time τ_s in Coulomb collisions (see Fig. 8d). Negative velocity differences are observed in streams from coronal streamers, in disturbed fast streams, and possibly in the heliospheric current sheet. It is important to note that the velocity differences in streams originating from streamers is negative, despite the large number and high efficiency of Coulomb collisions (i.e., the time ratio τ_e/τ_s) in these streams.

On the whole, the behavior of the relative velocity difference $(V_\alpha - V_p)/V_A$ on the concentration–velocity plane is similar to that of the simple velocity difference $V_\alpha - V_p$ (see Fig. 8c).

[1]These equations give the ratios of the flux propagation time τ_e to the characteristic times of energy transfer τ_c and momentum transfer τ_s in Coulomb collisions.

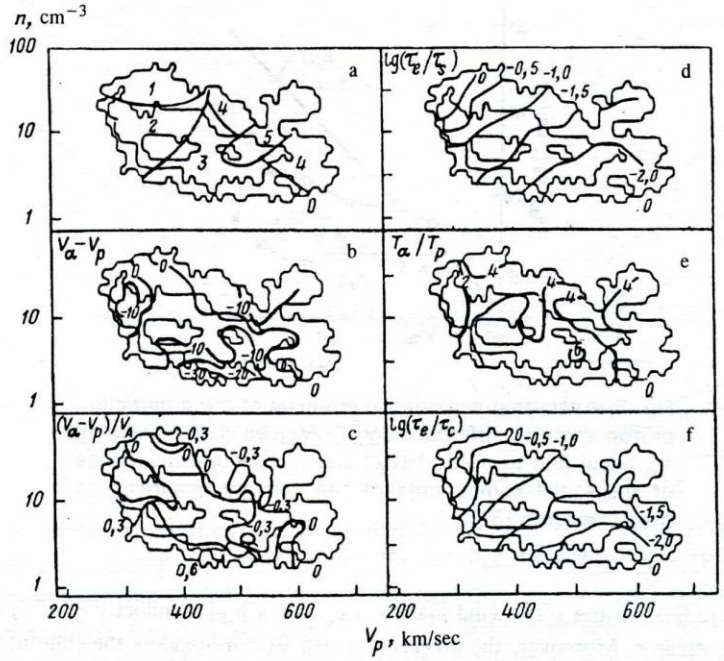

Fig. 8. Distribution maps on the concentration–velocity plane according to Prognoz-7 measurements [43, 54]: a) five types of solar wind streams (see text); b) α-particle–proton velocity difference $V_\alpha - V_p$; c) α-particle–proton velocity difference divided by Alfvén velocity $V_\alpha - V_p/V_A$; d) time ratio τ_e/τ_s [see Eq. (2)]; e) α-particle–proton temperature ratio T_α/T_p; f) time ratio τ_e/τ_c [see Eq. (1)].

High temperature ratios T_α/T_p are observed for the most part in streams from coronal holes, where the degree of departure from thermodynamic equilibrium increases with decreasing concentration on account of the decrease in the ratio of τ_e to τ_c (see Fig. 8f). Small temperature ratios are detected in streams from streamers, we well as partially in disturbed fast streams and in the heliospheric current sheet.

Even though the relationship of the velocities and temperatures of α-particles and protons to the types of solar wind streams as determined from Prognoz-7 satellite data agrees in part with previous results, the conclusions still need additional confirmation based on results from other space experiments.

2.2. Causes of Departure from Thermodynamic Equilibrium of the Components

It has been hypothesized in several theoretical papers that the mixing of streams having different velocities and different abundances of heavy ions will necessarily create a difference between the velocities of the components [74, 75]. The above data on the correlation of the helium abundance and the α-particle–proton velocity difference with the solar wind velocity supports this hypothesis. Indeed, if two streams with velocities $V_1 = V_{\alpha 1} = V_{p1} \neq V_2 = V_{\alpha 2} = V_{p2}$ and abundances $(n_\alpha/n_p)_1 \neq (n_\alpha/n_p)_2$ are mixed, averaging over all particles yields the velocity difference between α-particles and protons

$$V_\alpha - V_p = \frac{n_{p1} n_{p2}}{(n_{\alpha 1} + n_{\alpha 2})(n_{p1} + n_{p2})} [(n_\alpha/n_p)_2 - (n_\alpha/n_p)_1](V_2 - V_1), \tag{3}$$

i.e., an increase in the helium abundance $(n_\alpha/n_p)_2 > (n_\alpha/n_p)_1$ with an increase in the velocity $V_2 > V_1$ will necessarily create a positive velocity difference between α-particles and protons, as has indeed been observed in experiments [37, 76, 77]. (This hypothesis is consistent with the assumption that fast plasma beams with a high helium abundance can be formed as a result of reconnection of the magnetic field in the solar atmosphere [20]). It must be noted, however, that the pres-

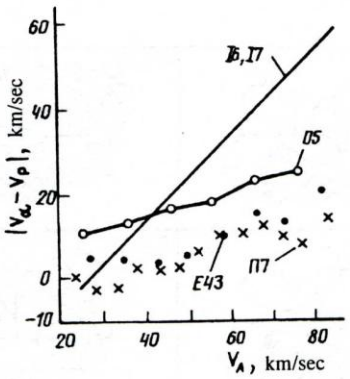

Fig. 9. Average graphs of the modulus of the α-particle–proton velocity difference $|\mathbf{V}_\alpha - \mathbf{V}_p|$ vs Alfvén velocity V_A according to data of [82] and the same dependence of the radial components of the velocity according to measurements [39].

ence of a frozen-in magnetic field in the solar wind plasma (i.e., for a high conductivity of the solar wind plasma) will prevent the mixing of such streams. Moreover, the presence of two streams renders the state of the plasma unstable, and the streams will mix on account of collective processes (including the evolution of plasma instabilities).

A profusion of models has been proposed to account for the observed departures from thermodynamic equilibrium of the proton and α-particle parameters in the solar wind, dealing with the predominant heating and acceleration of heavier ions as they interact with various types of waves in the solar wind (see, e.g., the surveys [4, 5] one of the latest original papers [78], along with the references cited in them). However, experimental data on this problem are scarce and conflicting [3–5, 76].

As mentioned, IMP 6 satellite data in a high-velocity stream have disclosed a correlation between the α-particle–proton velocity difference and the Alfvén velocity [57]. It has been deduced from Helios 1 and 2 spacecraft data that the velocity difference $V_\alpha - V_p$ in high-velocity streams at distances of ~ 0.3 AU attains equality with the Alfvén velocity, as opposed to earth orbit, where it is no more than $\sim 0.5 V_A$ [79]. It has been hypothesized on the basis of these data that α-particles are accelerated by Alfvén waves near the sun and by the subsequent equalization of the ion velocities at large heliocentric distances [80, 79], but a detailed comparison of this conjecture with experimental data has not been carried out. Consequently, the experimental dependences of the velocity difference $V_\alpha - V_p$ and the temperature ratio T_α/T_p on the Alfvén velocity are of special interest.

Figure 9 shows average curves of $V_\alpha - V_p$ as a function of V_A according to IMP 6 and 7, OGO 5, Explorer 43 [81], and Prognoz-7 [39] data. The Prognoz-7 data differ from the other experiments in that they represent the scalar α-particle–proton velocity difference measured along the earth–sun line. In the range of Alfvén velocities 20–80 km/sec the averaged velocity differences based on the Explorer 43 and Prognoz-7 experimental results are fairly close to one another and are about 5–10 km/sec lower than the values obtained from the OGO 5. On the other hand, the data from these three satellites differ appreciably from the average dependence (solid curve) obtained from the IMP 6 and 7 satellites for the fast stream 30.III–2.IV 1971.

To all appearances, only in certain types of solar wind streams (e.g., in certain high-velocity streams) are the values of the α-particle–proton velocity difference observed to be close to the Alfvén velocity. In other types of streams such a correlation is either very weak or is nonexistent. Consequently, the average dependences (see Fig. 9) are situated lower and have a smaller slope than those observed in individual events. Future investigations should be aimed at elucidating the conditions influencing this correlation.

The dependence of the α-particle–proton temperature ratio T_α/T_p on the Alfvén velocity has been investigated only according to data from the Prognoz-7 satellite [39] (see Fig. 10) an is analogous in its general features to the variation of the velocity difference in Fig. 9: As the Alfvén velocity increases from 15 km/sec to 75 km/sec, the average temperature ratio increases from ~ 1 to ~ 5 and then, despite an increase in the statistical scatter with a further increase of V_A to 120 km/sec, remains at this level on the average.

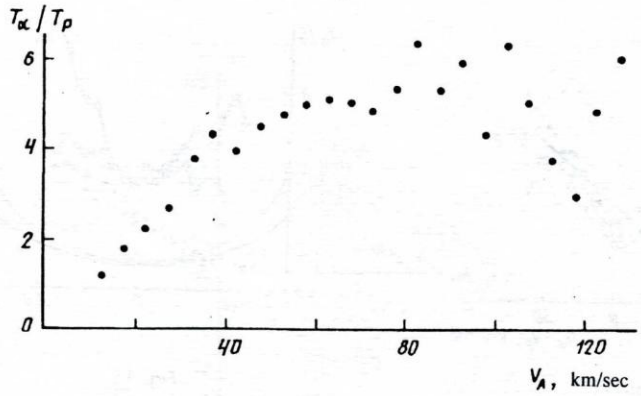

Fig. 10. Average graphs of the α-particle–proton temperature ratio T_α/T_p vs Alfvén velocity V_A according to Prognoz-7 measurements [39].

Thus, the results of spacecraft measurements do not present unequivocal evident in support of the mechanisms of the acceleration and heating of α-particles by Alfvén waves. We note that the Alfvén velocity can be calculated formally for any conditions in the solar wind, but in reality Alfvén waves (and these mechanisms) occur only under certain conditions in the solar wind. For example, Explorer 34 data [56] have revealed that periods in which a large velocity difference $V_\alpha - V_p$ is detected do not usually coincide with periods of elevated Alfvén wave levels in the solar wind. The relative level of oscillations of the hourly-average components of the magnetic field $\Delta B/B$ anticorrelate with the relative velocity difference $(V_\alpha - V_p)/V_A$ determined from OGO 5 and Explorer 43 data [3]. The dependences of the heating and acceleration of α-particles on the Alfvén velocity appear to be essentially circumstantial.

Additional information about the reasons for the loss of thermodynamic equilibrium between protons and α-particles can be obtained by studying the relationship between the predominant acceleration of α-particles and their predominant heating. Figure 11 shows the α-particle–proton temperature ratio T_α/T_p as a function of their velocity difference $V_\alpha - V_p$ according to space experiments on board the satellites IMP 6 (for the period 14.IV–26.VII 1972, open circles), OGO 5 ($\times$'s), IMP 6–8 {approximated by the relation $T_\alpha/T_p = (0.042 \pm 0.011)(V_\alpha - V_p)$[km/sec] + (4.5 ± 0.4)} [82, 81], and Prognoz-7 (dots) [37, 76, 39, 77].

These five satellites indicate a direct correlation between the parameters T_α/T_p and $V_\alpha - V_p$ in the interval of $V_\alpha - V_p$ from 0 to 70 km/sec. Moreover, Prognoz-7 data for $V_\alpha - V_p < -10$ km/sec show that T_α/T_p increases as $V_\alpha - V_p$ decreases; data in the range $V_\alpha - V_p < -20$ km/sec are lacking in other experiments. We note that OGO 5 data [82] definitely indicate a growth of T_α/T_p from ~ 3.9 at $V_\alpha - V_p = 0$ to ~ 4.4 at $V_\alpha - V_p = -20$ km/sec. Since the Prognoz-7 observations in the interval $V_\alpha - V_p = -20$ km/sec were comparatively few in number (roughly 1300 out of 11,000), the approximation of the Prognoz-7 data by a linear function over the entire range of velocity differences gives a positive correlation $T_\alpha/T_p = 0.04(V_\alpha - V_p) + 4.2$ [39], which is very close to the dependence obtained from the IMP 6–8 satellites. It can be concluded from the Prognoz-7 data, on the whole, that the temperature ratio T_α/T_p correlates with the modulus of the α-particle–proton velocity difference $|\mathbf{V}_\alpha - \mathbf{V}_p|$ in the solar wind, and the results of observations on different satellites are quite consistent with one another in the range of parameters where data are available from other space experiments. All the same, it is important to verify this conclusion on the basis of data from independent experiments.

A kinetic analysis in a theoretical paper [83] has disclosed evidence that friction forces between ion distributions separated from each other in velocity space tend to heat up both components in such a way as to change the temperature ratio T_α/T_p from ~ 1 at a small velocity difference $V_\alpha - V_p$ to a value $\sim (m_p n_p)/(m_\alpha n_\alpha) \approx 6$ (for $n_\alpha/n_p = 4\%$) at a large velocity difference.

To provide a quantitative comparison of the Prognoz-7 measurement results with the model, Fig. 12 shows the temperature ratio T_α/T_p as a function of the α-particle–proton velocity difference normalized to the average thermal velocity of the two particles $X = (V_\alpha - V_p)/W_T = (V_\alpha - V_p)/[2k(T_\alpha/m_\alpha + T_p/m_p)]^{1/2}$ for two sets of two intervals each: light symbols for a collisionless plasma ($\tau_e/\tau_c < 10^{-1}$), dark symbols for a collisional plasma ($\tau_e/\tau_c > 10^{-1}$), circles for

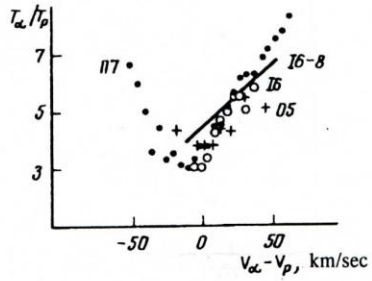

Fig. 11

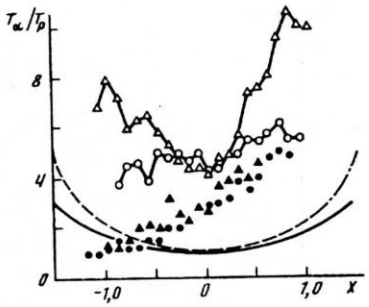

Fig. 12

Fig. 11. Average graphs of the α-particle–proton temperature ratio T_α/T_p vs their velocity difference $V_\alpha - V_p$ according to data from space experiments on the satellites IMP 6 (for the period 14.IV–26.VII 1972, open circles), OGO 5 (×'s), IMP 6–8 {approximated by the relation T_α/T_p = (0.042 ± 0.011)$(V_\alpha - V_p)$[km/s] + (4.5 ± 0.4)} [82, 81], and Prognoz-7 (dots) [37, 76, 39, 77].

Fig. 12. Average graphs of the α-particle–proton temperature ratio T_α/T_p vs their relative velocity difference $X = (V_\alpha - V_p)/[2k(T_\alpha/m_\alpha + T_p/m_p)]^{1/2}$ for two sets of two intervals (see text).

a plasma with a low helium abundance ($n_\alpha/n_p < 4\%$), and triangles for a plasma with a high helium abundance ($n_\alpha/n_p > 4\%$). Also shown in the figure are the results of model calculations [83] for $n_\alpha/n_p = 5\%$ (solid curve) and $n_\alpha/n_p = 2.5\%$ (dashed curve).

In a collisional plasma the difference between streams with small and large helium abundances is insignificant, and the average temperature ratio increases from ~1 to ~4 as the relative velocity difference increases from −1.0 to +0.7. The difference between such streams becomes significant in a collisionless plasma: The temperature ratio increases from ~4 to ~5 as X increases from −1.0 to +1.0 in streams with a small helium abundance, whereas in streams with a large helium abundance the temperature ratio decreases from ~7 to ~4 as X increases from −1.0 to 0, and it increases from ~4 to ~10 as X increases from 0 to +1.0. The conclusions drawn from the model of [83], which was developed for a collisional plasma (i.e., for dense and slow streams), do not concur with the results of Prognoz-7 measurements: First, a dependence of the temperatures T_α/T_p on the helium abundance n_α/n_p is not observed and, second, the temperature ratio depends on the sign of X. Only in collisionless streams with a high helium abundance, i.e., mainly in streams from coronal holes, is the temperature ratio observed to increase with the absolute value of the relative velocity difference $|X| = |V_\alpha - V_p|/W_T$.

The fact that the measured values of T_α/T_p are much higher, on the average, than the values calculated from the model of [83] shows that additional α-particle heating mechanisms exist in the solar wind. It can be assumed that the predominant heating of α-particles, in particular, is a consequence of the development of oscillations (instabilities) associated with the difference between the α-particle and proton velocities.

2.3. Equalization of Velocities and Temperatures of the Ion Components

The presence of oscillations and waves ("phonons") in the solar wind leads to scattering of the plasma particles and the equalization of their macroscopic parameters, and thermodynamic disequilibrium between protons and α-particles (and other heavy ions) can excite these oscillations. Similar particle scattering can be caused by the existence of hydrodynamic discontinuities in the solar wind. The influence of the sun's rotation is such as to diminish the difference between the proton and α-particle velocities [3].

Coulomb collisions have been postulated as one of the possible mechanisms equalizing the transport velocities and kinetic temperatures of α-particles and protons in the solar wind. To test this hypothesis, experimental data have been used to investigate the dependences of the velocity difference $V_\alpha - V_p$ and the relative velocity difference $(V_\alpha - V_p)/V_A$ on the time ratio τ_e/τ_s and of the temperature ratio T_α/T_p on the time ratio τ_e/τ_c. The primary data, obtained from the

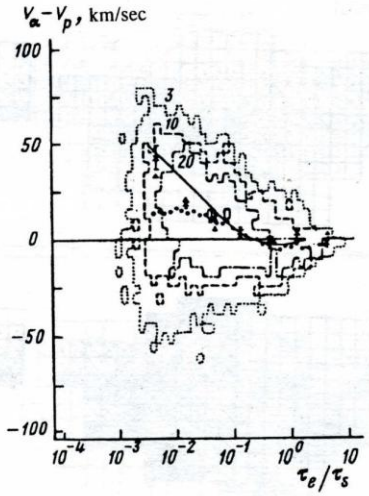

Fig. 13. Average graphs of the α-particle – proton velocity difference $V_\alpha - V_p$ vs the time ratio τ_e/τ_s [see Eq. (2)] according to measurements on the satellites OGO 5 [85] (×'s), Heos 2 [60] (solid curve), Explorer 43 [3] (triangles), and Prognoz-7; the primary data are represented by isographs of $N > 3$ (dashed line), >10 (dotted line), >20 (dot-dashed line), and >65 (solid line) measurements in the unit cell, and the averaged data are represented by heavy dots [37, 39, 76, 77].

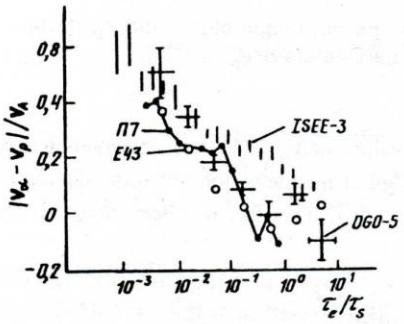

Fig. 14

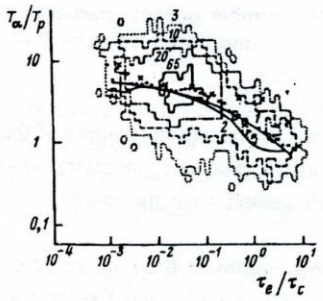

Fig. 15

Fig. 14. Average graphs of the relative α-particle – proton velocity difference $V_\alpha - V_p/V_A$ vs the time ratio τ_e/τ_s according to measurements on several spacecraft.

Fig. 15. Average graphs of the α-particle – proton temperature ratio T_α/T_p vs the time ratio τ_e/τ_c [see Eq. (1)] according to measurements on the satellites OGO 5 (×'s) [84], IMP 6 (curve 1) [86], ISEE 3 (curve 2) [68], and Prognoz-7 (the notation is the same as in Fig. 13) [37, 39, 76, 77].

Prognoz-7 satellite [37, 39, 75, 77], are represented in Figs. 13 and 15 by isographs of constant values of the number of measurements in the unit cell: $N > 3$ (dashed lines); $N > 10$ (dotted lines); $N > 20$ (dot-dash lines); $N > 65$ (solid lines); averaged data (circles). Figure 13 also shows the results of determining the average dependence of $V_\alpha - V_p$ on the ratio τ_e/τ_s according to measurements on board the OGO 5 [85] (×'s), the Heos 2 [60] (solid curve), and the Explorer 43 [3] (triangles). In addition to a systematic decrease in the average value of $V_\alpha - V_p$ as τ_e/τ_s increases, two other facts come to light: First, on the average, α-particles move more slowly than protons in a collisional solar wind plasma

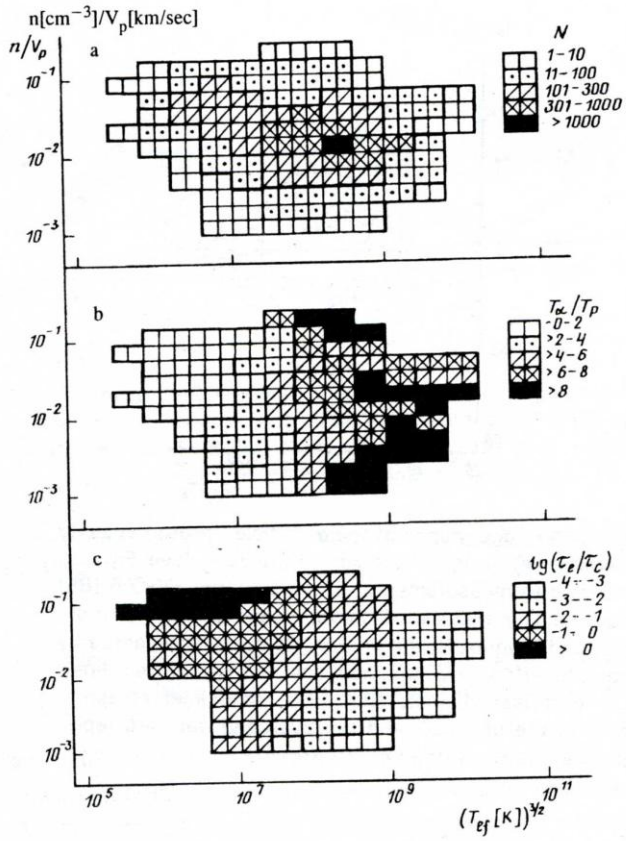

Fig. 16. Number of measurements N (a), α-particle–proton temperature ratio T_α/T_p (b), and time ratio τ_e/τ_c [see Eq. (1)] (c) vs parameters n/V_p and T_{ef}.

($\tau_e/\tau_s \geq 1$) and, second, the deviation (scatter) of the experimental values of $V_\alpha - V_p$ from the averages, observed on the Prognoz-7, decreases as the ratio τ_e/τ_s increases, regardless of the sign of this deviation (even though the number of cases with $V_\alpha > V_p$ is much greater than the number of cases with $V_\alpha < V_p$). This fact has been noted in Heos 2 measurements [81].

Figure 14 shows graphs of the relative velocity difference $(V_\alpha - V_p)/V_A$ on the ratio τ_e/τ_s according to measurements on the satellites OGO 5 ($\times$'s) and Explorer 43 (circles) [3], ISEE 3 (vertical segments) [68], and Prognoz-7 (dots) [39]. The behavior of $(V_\alpha - V_p)/V_A$ resembles the variation of $V_\alpha - V_p$, but Prognoz-7 data [39] show that the scatter of $(V_\alpha - V_p)/V_A$ about the average, unlike $V_\alpha - V_p$, is roughly constant over the entire range of the time ratio τ_e/τ_s.

Graphs of the temperature ratio T_α/T_p as a function of the time ratio τ_e/τ_c according to measurements on the satellites OGO 5 ($\times$'s) [84], IMP 6 (curve 1) [86], and ISEE 3 (curve 2) [68] are compared in Fig. 15 with Prognoz-7 measurements of protons and α-particles (dots) [76]. The results of all four experiments are in good agreement and indicate that the temperature ratio T_α/T_p decreases to ~ 1 as the time ratio τ_e/τ_c increases.

The data shown in Figs. 13–15 from different space experiments do not contradict the hypothesis that Coulomb collisions play some part in the velocity and temperature equalization of different ion components of the solar wind; strictly speaking, however, they cannot be regarded as conclusive evidence in support of the hypothesis that Coulomb collisions are in fact the decisive factor. The problem is that the time ratios τ_e/τ_s and τ_e/τ_c include the factor n/V_p, which can be interpreted as a parameter characterizing the "number of collisions" of any kind whatsoever and which varies by more than two orders of magnitude in the solar wind. To determine the nature of the collisions, it is necessary to investigate the dependence of the velocity difference and temperature ratio of α-particles and protons on other, slightly varying parameters against the background of the extremely variable parameter n/V_p.

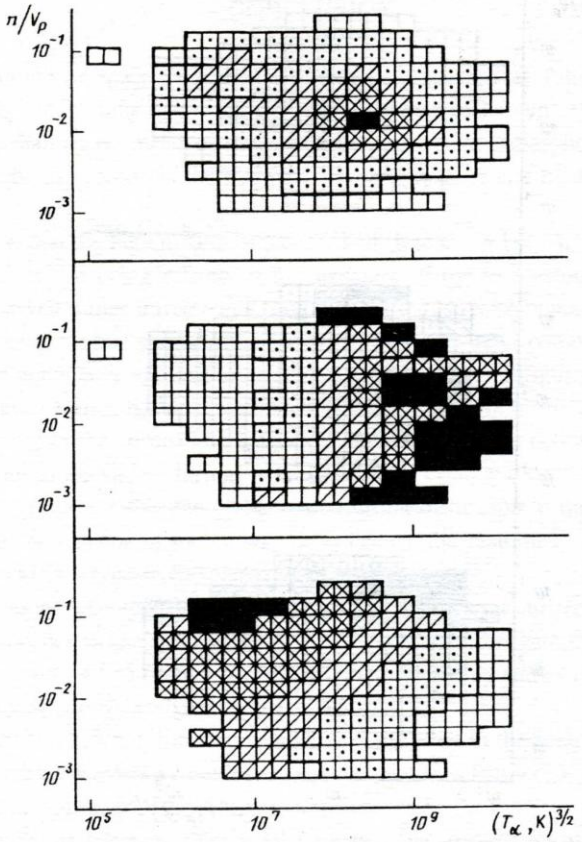

Fig. 17. The same as Fig. 16, but for T_α instead of T_{ef}.

Such an attempt has been made on the basis of data from the spacecraft ISEE 3 [68] in an investigation of the dependence of T_α/T_p on T_{ef} [see Eq. (1)] using data grouped selectively by intervals of n/V_p. The ratio T_α/T_p increases with T_{ef} for all intervals of n/V_p, in qualitative agreement with Eq. (1). However, no discrepancies were observed for the curves of T_α/T_p versus T_{ef} in different intervals of n/V_p, i.e., a dependence on the parameter n/V_p could not be discerned.

We have studied this problem in closer detail, using Prognoz-7 data, and the results are presented in Figs. 16–18, which show two-dimensional (bivariate) graphs of the number of measurements (a), the temperature ratio T_α/T_p (b), and the time ratio τ_e/τ_c (c) as functions of the parameter n/V_p and the temperature. Figures 16–18 differ in the abscissas, which represent $T_{ef}^{3/2}$, $T_\alpha^{3/2}$, and $T_p^{3/2}$, respectively, in logarithmic scale. Figure 16b shows results similar to those obtained from the ISEE 3: The ratio T_α/T_p increases with T_{ef} in different intervals of n/V_p, but a significant dependence of T_α/T_p on n/V_p is not observed. Moreover, we note that this is true of both collisional and collisionless plasmas (see Fig. 16c). A similar result is obtained in Fig. 17. It is most likely attributable to the fact that T_{ef} varies from $0.8T_\alpha$ to $1.0T_\alpha$ according to Eq. (1), so that Fig. 16 mainly reflects the behavior of the parameters as T_α varies.

Figure 18 differs radically from Figs. 16 and 17: On the whole, the temperature ratio T_α/T_p decreases as T_p increases (without any appreciable dependence on n/V_p), but is small only in a narrow interval for a collisional plasma ($T_p^{3/2} < 10^7$, and $n[\text{cm}^{-3}]/V_p[\text{cm/sec}] \sim 0.1$), where it can be stated – although with due caution owing to the limited statistics – that the temperature ratio T_α/T_p decreases with increasing value of n/V_p in a collisional plasma. In a collisionless plasma the variation of T_α/T_p with T_α (as with T_{ef}) and T_p is consistent with the law that T_α/T_p is proportional to T_α, inversely proportional to T_p, and independent of n/V_p. Consequently, neither an analysis based on data from the ISEE 3 spacecraft [68] or the above analysis offers any new arguments in favor of the hypothesis that Coulomb collisions *per se* play a preeminent role in equalizing the temperatures of the ion components in the solar wind.

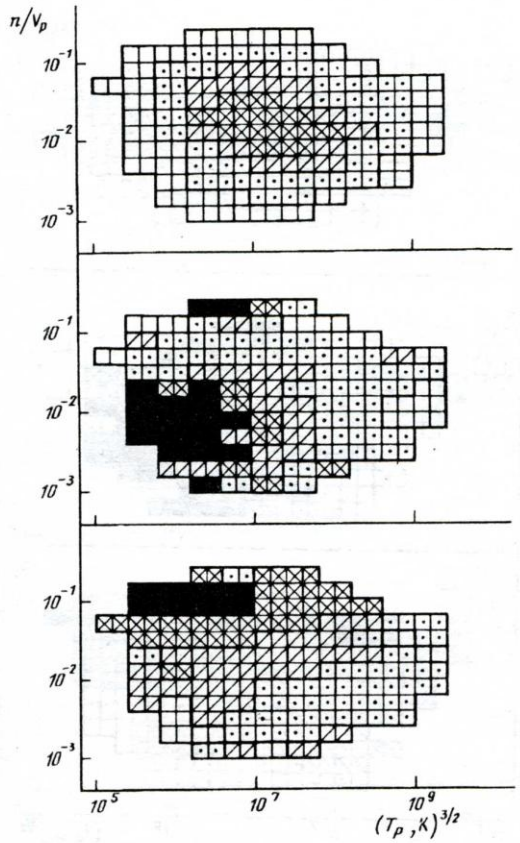

Fig. 18. The same as Fig. 16, but for T_p instead of T_{ef}.

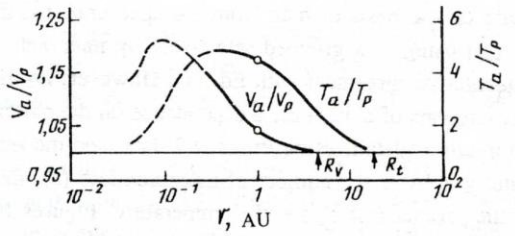

Fig. 19. Average graphs of the α-particle – proton velocity ratio V_α/V_p and temperature ratio T_α/T_p vs heliocentric distance [39, 76, 77].

The analysis of Prognoz-7 data in Figs. 13–15 and the several conjectures about the variation of the hydrodynamic parameters of the solar wind with varying heliocentric distance have led to the hypothesis that the velocities and temperature of α-particles and protons equalize, on the average, at a distances of ~7 AU and 20 AU, respectively [76, 39, 77]. Figure 19 shows schematically the velocity and temperature dynamics of α-particles relative to protons with increasing heliocentric distance. Direct measurements at distances shorter than 0.3 AU (dashed segments of the curves) do not exist at the present time. Helium measurements at distances greater than 1 AU have been performed, for example, on the Voyager 2 and Pioneer 11 spacecraft (moving at distances greater than 30 AU) and also on the Pioneer 10 (beyond 50 AU), but the data have not yet been published.

CONCLUSION

The data from a multitude of space experiments can be summarized as follows. Helium in the solar wind is detected mainly in the form of $^4He^{++}$ ions (α-particles). The abundance of helium relative to protons n_α/n_p in the solar wind is lower, on the average, than all estimates of its abundance in the solar atmosphere, but is considerably higher than predicted by models that describe the corona in the hydrostatic approximation and treat it as a boundary condition for the formation of the solar wind.

The measurements show that the helium abundance in small time scales (< 1 h) varies from one type of solar wind stream to another, the type of stream being related to the structure of (or to phenomena in) the solar corona. A high helium abundance $> 9\%$ is observed rather infrequently, and then only in streams containing plasma ejected from the solar atmosphere during powerful transient phenomena (solar flares, storms, and other comparatively short-lived processes). In quasisteady streams the helium abundance appears to depend strongly on the configuration of the coronal magnetic field, having values of 4–6% in streams originating from regions with a field structure of the coronal hole type, 2–4% in streams from regions with a field structure of the coronal streamer type, and $\sim 1\%$ in the heliospheric current sheet.

The average helium abundance varies during the solar activity cycle and correlates with the number of sunspots. This is most likely attributable to the fact that the global restructuring of the sun in the solar cycle alters the structure of the coronal magnetic field near the equator in such a way as to change the relationship between the durations of different types of streams in the solar wind observed from spacecraft near the ecliptic.

The experimental data support an approach operating on the principle that to arrive at a satisfactory explanation for the observations of helium abundance in the solar wind, it is necessary to investigate the problems of coronal heating and the genesis of the solar wind from a unified point of view, i.e., to study the dynamics of the multicomponent plasma from the upper part of the photosphere out to interplanetary space [86, 87].

Thermodynamic equilibrium between ion components does not exist in the solar wind at small heliocentric distances $r \leq 1$ AU: On the average, the α-particle velocities exceed the proton velocities, $V_\alpha > V_p$, and their temperature ratio T_α/T_p is close to 4. Earth orbit measurements show that the ratios between the transport velocities and kinetic temperatures of α-particles are associated with the types of solar wind streams. The greatest departure from equilibrium is observed mainly in streams from coronal holes, where the α-particle velocity usually exceeds the proton velocity by an amount of the order of the Alfvén velocity, and their temperature ratio is equal to 3–6. The smallest departure occurs in streams from coronal streams and in the heliospheric current sheet, where the α-particle velocities are equal to or slightly smaller than the proton velocities, and their temperature ratio is equal to 0.8–3. Observations at small heliocentric distances of 0.3–1.0 AU show that equilibrium is probably lost at even shorter distances ($r \leq 0.3$ AU).

The most probable scenario of the dynamics of the parameters of protons and α-particles is the following. First, a shift takes place between the proton and α-particle distribution functions in velocity space. This effect can be caused by reconnection of the magnetic fields at the level of the photosphere, whereupon beams are formed in the corona with a large helium abundance and a velocity exceeding that of the surrounding plasma by an amount equal to the local Alfvén velocity. On the one hand, these beams can heat the corona through their interaction with the surrounding plasma and, on the other, the waves generated by them can heat the ion components to equal thermal velocities (or their temperature ratio is proportional to their mass ratio) [86, 87]. Moreover, the α-particle and proton distribution functions in velocity space can be caused to shift by the mixing of streams having different velocities and different helium abundances [74, 75, 77]. Subsequently, the energy embodied in the velocity difference causes the thermal velocities of the ion components to increase and equalize (i.e., T_α tends to $4T_p$), and the difference between the transport velocities of the components decreases. The transport velocities and kinetic temperatures finally tend to equalize at large heliocentric distances (the former at $r \sim 7$ AU) and the latter at $r \sim 20$ AU) [77].

In closing, the author would like to thank G. N. Zastenker for a valuable discussion of the content of the article and M. Yu. Ermolaev for assisting with the preparation of the manuscript for publication.

This work has been supported in part by a Soros Humanitarian Foundations Grant awarded by the American Physical Society.

LITERATURE CITED

1. M. Neugebauer and C. W. Snyder, "The mission of Mariner 2: planetary observation; solar plasma experiment," Science, **138**, 1095 (1962).
2. M. Neugebauer and C. W. Snyder, "Mariner 2 observation of the solar wind. 1. Average properties," J. Geophys. Res., **71**, 4469 (1966).
3. M. Neugebauer, "Observation of solar wind helium," Fund. Cosmic Phys., **7**, 131 (1981).
4. I. S. Veselovskii, Physics of the Interplanetary Plasma (Progress in Science and Technology: Space Research, Vol. 22) [in Russian], VINITI, Moscow (1984).
5. Yu. I. Ermolaev, "Large-scale characteristics of the ion component of the solar wind according to the results of spacecraft measurements," IKI AN SSSR Preprint No. 1281 [in Russian], Space Research Institute, Academy of Sciences of the USSR, Moscow (1987).
6. B. Z. Kozlovsky, "The stages of ionization of oxygen and helium in the solar wind," Solar Phys., **5**, 410 (1968).
7. J. T. Gosling, J. R. Asbridge, S. J. Bame, et al., "Observations of large fluxes of He^+ in solar wind following an interplanetary shock," J. Geophys. Res., **85**, 3431 (1980).
8. R. Schwenn, H. Rosenbauer, and K.-H. Muhlhauser, "Singly-ionized helium in the driver gas of an interplanetary shock," Geophys. Res. Lett., **7**, No. 3, 201 (1980).
9. R. D. Zwickl, J. R. Asbridge, S. J. Bame, W. C. Feldman, J. T. Gosling, "He^+ and other unusual ions in the solar wind: a systematic search covering 1972–1980," J. Geophys. Res., **87**, No. 9, 7379 (1982).
10. N. F. Pisarenko, E. M. Dubinin, A. V. Zakharov, et al., "Observation of He^+ ions in the solar wind," J. Geophys. Res., **90**, No. 5, 4367 (1985).
11. Yu. I. Ermolaev, V. I. Zhuravlev, G. N. Zastenker, et al., "Observations of singly-ionized helium in the solar wind," Kosm. Issled., **27**, No. 5, 717 (1989).
12. P. Bochsler, J. Geiss, and A. Maeder, "The abundance of ^3He in the solar wind – a constraint for models of solar evolution," Solar Phys., **128**, 203 (1990).
13. M. Neugebauer, "Measurements of the properties of solar wind plasma relevant to study of its coronal sources," Space Sci. Rev., **33**, 127 (1982).
14. K. W. Ogilvie and T. D. W. Wilkerson, "Helium abundance in the solar wind," Solar Phys., **8**, No. 2, 435 (1969).
15. M. A. Coplan, K. W. Ogilvie, P. Bochsler, and J. Geiss, "Ion composition instrument," IEEE Trans. Geosci. Electron., **GE-16**, 185 (1978).
16. O. L. Vaisberg, L. S. Gorn, Yu. I. Ermolaev, et al., "Experiment in interplanetary and magnetospheric plasma diagnostics on the interplanetary probes Venera-11, 12 and the satellite Prognoz-7," Kosm. Issled., **17**, No. 5, 780 (1978).
17. V. Formisano and G. Moreno, "Helium and heavy ions in the solar wind," Rev. Nuovo Cimento, **1**, 365 (1971).
18. A. Bürgi and J. Geiss, "Helium and minor ions in the corona and solar wind: dynamics and charge states," Solar Phys., **103**, 347 (1986).
19. D. E. Robbins, A. J. Hundhausen, and S. J. Bame, "Helium in the solar wind," J. Geophys. Res., **75**, No. 7, 1176 (1970).
20. W. C. Feldman, "Signatures of small solar transients in the solar wind," in: The Sun, Solar Wind, and Near Earth Processes, Soviet–American Workshop on Solar-Terrestrial Physics (Abstracts), Dagomys, USSR (October 15–20, 1990), p. 7.
21. A. J. Hundhausen, Solar Wind and Coronal Expansion, Springer-Verlag, New York (1972).
22. D. L. Lambert, "Abundance of helium in the sun," Nature, **215**, 43 (1967).
23. A. J. Hundhausen, J. R. Asbridge, S. Bame, et al., "Vela 3 satellite observations of solar wind ions: a preliminary report," J. Geophys. Res., **72**, 87 (1967).
24. V. Formisano, F. Palmiotto, and G. Moreno, "α-Particle observations in the solar wind," Solar Phys., **15**, No. 2, 479 (1970).
25. J. Hirshberg, S. J. Bame, and D. E. Robbins, "Solar flares and solar wind helium enrichments: July 1965 – July 1967," Solar Phys., **23**, No. 2, 467 (1972).

26. K. W. Ogilvie, "Helium abundance variations," J. Geophys. Res., **77**, 4227 (1972).
27. G. Moreno and F. Palmiotto, "Variations of α-particle abundance in the solar wind," Solar Phys., **30**, 207 (1973).
28. K. W. Ogilvie and J. Hirshberg, "The solar cycle variation of the solar wind helium abundance," J. Geophys. Res., **79**, 4595 (1974).
29. S. J. Bame, J. R. Asbridge, W. C. Feldman, and J. T. Gosling, "Evidence for a structure-free state at high solar wind speeds," J. Geophys. Res., **92**, No. 10, 1487 (1977).
30. W. C. Feldman, J. R. Asbridge, S. J. Bame, and J. T. Gosling, "Long-term variations of selected solar wind properties: IMP 6, 7, and 8 results," J. Geophys. Res., **83**, No. 5, 2177 (1978).
31. R. Schwenn, "The 'average' solar wind in the inner heliosphere structure and slow variations," in: Solar Wind Five, M. Neugebauer (ed.), NASA Conference Publication 2280 (1983), p. 489.
32. S. J. Bame, "Solar wind minor ions – recent observations," in: Solar Wind Five, M. Neugebauer (ed.), NASA Conference Publication 2280 (1983), p. 573.
33. Yu. I. Ermolaev, V. V. Stupin, G. N. Zastenker, et al., "Variations of the hydrodynamic parameters of solar wind protons and α-particles according to data from selective measurements on the Prognoz-7 satellite," IKI AN SSSR Preprint No. 1357 [in Russian], Space Research Institute, Academy of Sciences of the USSR, Moscow (1988).
34. K. W. Ogilvie, M. A. Coplan, P. Bochsler, and J. Geiss, "Solar wind observations with ion composition instrument aboard the ISEE 3 ICE spacecraft," Solar Phys., **124**, 167 (1989).
35. D. Bollea, V. Formisano, P. C. Hedgecock, et al., "Heos-1 helium observations in the solar wind," in: Solar Wind, NASA P-308 (1972).
36. J. Feynman, "Solar cycle and long term changes in the solar wind," Rev. Geophys. Space Phys., **21**, 338 (1983).
37. Yu. I. Ermolaev, V. V. Stupin, G. N. Zastenker, et al., "Variations of the hydrodynamic parameters of solar wind protons and α-particles according to measurements on the Prognoz-7 satellite," Kosm. Issled., **28**, No. 2, 218 (1990).
38. J. Hirshberg, J. R. Asbridge, and D. E. Robbins, " Velocity and flux dependence of solar wind abundance," J. Geophys. Res., **77**, 3583 (1972).
39. Yu. I. Yermolaev [Ermolaev], G. N. Zastenker, and V. V. Stupin, "Relationships between bulk parameters of solar wind protons and alpha-particles: Prognoz-7 measurements," Preprint No. 1575, Space Research Institute, Academy of Sciences of the USSR, Moscow (1990).
40. Yu. I. Ermolaev and V. V. Stupin, " Relationship of helium abundance to solar wind conditions according to measurements on the Prognoz-7 satellite," Kosm. Issled., **28**, No. 4, 571 (1990).
41. J. Geiss, P. Hirt, and H. Leutwyler, "On acceleration and motion of ions in corona and solar wind," Solar Phys., **12**, 458 (1970).
42. J. T. Gosling, G. Borrini, J. R. Asbridge, et al., "Coronal streamers in the solar wind at 1 AU," J. Geophys. Res., **86**, No. 7, 5438 (1981).
43. Yu. I. Yermolaev [Ermolaev], "Large-scale structure of solar wind and its relationship with solar corona: Prognoz-7 observations," Planet. Space Sci., **39**, No. 10, 1351 (1991).
44. W. C. Feldman, J. R. Asbridge, S. J. Bame, et al., "The solar origins of solar wind interstream flows: near-equatorial corona streamers," J. Geophys. Res., **86**, No. 7, 5408 (1981).
45. Yu. I. Yermolaev [Ermolaev], "Mass, momentum, and energy transport from the Sun to the Earth by different types of the solar wind: Prognoz-7 observations," in: Proceedings of the 26th ESLAB Symposium on Study of the Solar-Terrestrial System, Killarney, Ireland, ESA SP-346 (1992), p. 217.
46. L. F. Burlaga and K. W. Ogilvie, "Heating of the solar wind," Astrophys. J., **159**, No. 2, 659 (1970).
47. S. J. Bame, J. R. Asbridge, A. J. Hundhausen, and I. B. Strong, "Solar wind and magnetosheath observations during the January 13–14, 1967 geomagnetic storm," J. Geophys. Res., **73**, 5761 (1968).
48. S. J. Bame, J. R. Asbridge, W. C. Feldman, et al., "Solar wind heavy ions from flare-heated coronal plasma," Solar Phys., **62**, 179 (1979).
49. J. Hirshberg, A. Alksne, D. S. Colburn, et al., "Observations of a solar flare induced interplanetary shock and helium-enriched driver gas," J. Geophys. Res., **75**, 1 (1970).
50. E. E. Fenimore, "Solar wind flows associated with hot heavy ions," Astrophys. J., **235**, No. 1, 245 (1980).
51. G. Borrini, J. T. Gosling, S. J. Bame, et al., "Solar wind helium and hydrogen structure near the heliospheric current sheet," J. Geophys. Res., **86**, No. A6, 4565 (1981).

52. J. Hirshberg, J. R. Asbridge, and D. E. Robbins, "The helium component of solar wind, velocity streams," J. Geophys. Res., **79**, No. 7, 934 (1974).
53. G. T. Gosling, J. R. Asbridge, S. J. Bame, and W. C. Feldman, "Solar wind stream interfaces," J. Geophys. Res., **83**, 1401 (1978).
54. Yu. I. Ermolaev, "New approach to the investigation of the large-scale structure of the solar corona from measurements of solar wind parameters," Kosm. Issled., **28**, No. 6, 890 (1990).
55. K. W. Ogilvie and H. J. Zwally, "Hydrogen and helium velocities in solar wind," Solar Phys., **24**, 236 (1972).
56. K. W. Ogilvie, "Differences between the bulk speeds of hydrogen and helium in the solar wind," J. Geophys. Res., **80**, 1335 (1975).
57. J. R. Asbridge, S. J. Bame, W. C. Feldman, and M. D. Montgomery, "Helium and hydrogen velocity differences in the solar wind," J. Geophys. Res., **81**, No. 16, 2719 (1976).
58. A. A. Zertsalov, J. M. Bosqued, C. D'Uston, et al., "Results of Measurements of the α-component of the solar wind on the Prognoz satellite," Kosm. Issled., **14**, No. 3, 463 (1976).
59. J. M. Bosqued, C. D'Uston, A. A. Zertsalov, and O. L. Vaisberg, "Study of alpha component dynamics in the solar wind using Prognoz satellite," Solar Phys., **51**, 231 (1977).
60. H. Grunwaldt and H. Rosenbauer, "Study of helium and hydrogen velocity differences as derived from Heos 2 S-210 solar wind measurements," in: Plenum Feux sur la Physique Solaire 1979, Editions CNPS (1979), p. 377.
61. K. W. Ogilvie, M. A. Coplan, and R. D. Zwickl, "Helium, hydrogen, and oxygen velocities observed on ISEE 3," J. Geophys. Res., **87**, No. 9, 7363 (1982).
62. Yu. I. Ermolaev, "Behavior of the kinetic parameters of protons and α-particles as functions of the solar wind velocity," Kosm. Issled., **24**, No. 5, 725 (1986).
63. L. Avanov, N. Borodkova, Z. Nemecek, et al., "Some features of solar wind protons, α-particles, and heavy ions behavior: the Prognoz-7 and Prognoz-8 experimental results," Czech. J. Phys., **37**, No. 6, 759 (1987).
64. W. K. H. Schmidt, H. Rosenbauer, E. G. Shelley, and J. Geiss, "On temperature and speed of He^{++} and O^{6+} ions in the solar wind," Geophys. Res. Lett., **7**, No. 9, 697 (1980).
65. K. W. Ogilvie, P. Bochsler, J. Geiss, and M. A. Coplan, Observations of the velocity distribution of solar wind ions," J. Geophys. Res., **85**, No. A11, 6069 (1980).
66. P. Bochsler, J. Geiss, and R. Joos, "Kinetic temperatures of heavy ions in the solar wind," J. Geophys. Res., **90**, No. 11, 10779 (1985).
67. J. Feynman, "On solar wind helium and heavy ion temperatures," Solar Phys., **43**, No. 1, 249 (1975).
68. L. W. Klein, K. W. Ogilvie, and L. F. Burlaga, "Coulomb collisions in the solar wind," J. Geophys. Res., **90**, No. 8, 7389 (1985).
69. G. N. Zastenker, O. L. Vaisberg, V. M. Balebanov, et al., "Dynamics of solar wind plasma parameters and behaviour of magnetosphere boundaries during the arrival of interplanetary shock waves to the earth in the events of April–May, 1981," Preprint No. D 305, Space Research Institute, Academy of Sciences of the USSR, Moscow (1982).
70. G. N. Zastenker, N. L. Borodkova, O. L. Vaisberg, et al., "Interplanetary shock waves in the period after the solar maximum year: observation onboard the Prognoz-8 satellite," Preprint No. 841, Space Research Institute, Academy of Sciences of the USSR, Moscow (1983).
71. G. N. Zastenker and N. L. Borodkova, "Some features of the interplanetary disturbances in the post-solar maximum year period," Adv. Space Res., **4**, No. 7, 347 (1984).
72. G. N. Zastenker and N. L. Borodkova, "Interplanetary shocks in April–May, 1981," Kosm. Issled., **22**, No. 1, 87 (1984).
73. D. Spitzer, Jr., Physics of Fully Ionized Gases, 2nd ed., Wiley, New York (1962).
74. R. Steinitz and M. Eyni, "A model for the interaction of solar wind streams," in: COSPAR Symposium, Tel Aviv, 1977, M. A. Shea, D. F. Smart, and S. T. Wu (eds.) (1977), p. 101.
75. I. S. Veselovskii, "Evolution of strong inhomogeneities in the solar wind plasma," Geomagn. Aeron., **18**, No. 1, 3 (1978).
76. Yu. I. Yermolaev [Ermolaev] and V. V. Stupin, "Some alpha-particle heating and acceleration mechanisms in the solar wind: Prognoz-7 measurements," Planet. Space Sci., **38**, No. 10, 1305 (1990).

77. Yu. I. Yermolaev [Ermolaev], "Helium abundance, acceleration, and heating and large scale structure of the solar wind," in: Solar Wind Seven, COSPAR Colloquia Series 1991, Vol. 3, E. Marsch and R. Schwenn (eds.) (1992), p. 411.
78. L. Gomberff and R. Hernandez, "On the acceleration of alpha particles in the fast solar wind," J. Geophys. Res., **97**, No. A8, 12113 (1992).
79. E. Marsch, K.-H. Muhlhauser, H. Rosenbauer, R. Schwenn, and F. M. Neubeuer, "Solar wind helium ions: observation of the Helios solar probes between 0.3 and 1 AU," J. Geophys. Res., **87**, No. 1, 35 (1982).
80. J. V. Hollweg and J. M. Turner, "Acceleration of solar wind He^{++} effects of resonant and nonresonant interactions with transverse waves," J. Geophys. Res., **83**, 97 (1978).
81. M. Neugebauer, "Observations of solar wind helium," in: Solar Wind Four, H. Rosenbauer (ed.), Report No. MPAE-W-100-81-31 (1981), p. 425.
82. M. Neugebauer and W. C. Feldman, "Relation between superheating and superacceleration of helium in the solar wind," Solar Phys., **63**, 201 (1975).
83. R. Hernandez and E. Marsch, "Collisional time scales for temperature and velocity exchange between drifting Maxwellians," J. Geophys. Res., **90**, No. 11, 11062 (1985).
84. M. Neugebauer, "The role of Coulomb collisions in limiting differential flow and temperature differences in the solar wind," J. Geophys. Res., **81**, No. 1, 78 (1976).
85. W. C. Feldman, J. R. Asbridge, and S. J. Bame, "The solar wind He^{2+} to H^{+} temperature ratio," J. Geophys. Res., **79**, 2319 (1974).
86. W. I. Axford, and J. F. McKenzie, "The origin of high speed solar wind streams," in: Solar Wind Seven, COSPAR Colloquia Series 1991, Vol. 3, E. Marsch and R. Schwenn (eds.) (1992), p. 1.
87. J. V. Hollweg, "Status of solar wind modeling from the transition region outwards," in: Solar Wind Seven, COSPAR Colloquia Series 1991, Vol. 3, E. Marsch and R. Schwenn (eds.) (1992), p. 58.